THE JOURNAL OF PHYSICAL CHEMISTRY C

Subscriber access provided by University of Newcastle, Australia

Article

Silica Based Catalyst Supports Are Inert, Aren't They? – Striking Differences in Ethanol Decomposition Reaction Originated from Meso- & Surface Fine Structure Evidenced by Small Angle X-ray Scattering

András Sápi, Dorina G. Dobó, Daniel Sebok, Gyula Halasi, Koppány L. Juhász, Akos Szamosvölgyi, Peter Pusztai, Erika Varga, Ildikó Kálomista, Gábor Galbács, Akos Kukovecz, and Zoltán Kónya

J. Phys. Chem. C, **Just Accepted Manuscript** • DOI: 10.1021/acs.jpcc.7b00034 • Publication Date (Web): 17 Feb 2017

Downloaded from http://pubs.acs.org on February 20, 2017

Just Accepted

"Just Accepted" manuscripts have been peer-reviewed and accepted for publication. They are posted online prior to technical editing, formatting for publication and author proofing. The American Chemical Society provides "Just Accepted" as a free service to the research community to expedite the dissemination of scientific material as soon as possible after acceptance. "Just Accepted" manuscripts appear in full in PDF format accompanied by an HTML abstract. "Just Accepted" manuscripts have been fully peer reviewed, but should not be considered the official version of record. They are accessible to all readers and citable by the Digital Object Identifier (DOI®). "Just Accepted" is an optional service offered to authors. Therefore, the "Just Accepted" Web site may not include all articles that will be published in the journal. After a manuscript is technically edited and formatted, it will be removed from the "Just Accepted" Web site and published as an ASAP article. Note that technical editing may introduce minor changes to the manuscript text and/or graphics which could affect content, and all legal disclaimers and ethical guidelines that apply to the journal pertain. ACS cannot be held responsible for errors or consequences arising from the use of information contained in these "Just Accepted" manuscripts.

ACS Publications

The Journal of Physical Chemistry C is published by the American Chemical Society. 1155 Sixteenth Street N.W., Washington, DC 20036

Published by American Chemical Society. Copyright © American Chemical Society. However, no copyright claim is made to original U.S. Government works, or works produced by employees of any Commonwealth realm Crown government in the course of their duties.

Silica Based Catalyst Supports Are Inert, Aren't They? – Striking Differences in Ethanol Decomposition Reaction Originated from Meso- & Surface Fine Structure Evidenced by Small Angle X-ray Scattering

András Sápi[*,†,‡], *Dorina G. Dobó*[†,φ,‡], *Dániel Sebők*[ψ,‡], *Gyula Halasi*[†], *Koppány L. Juhász*[†], *Ákos Szamosvölgyi*[†], *Péter Pusztai*[†], *Erika Varga*[§], *Ildikó Kálomista*[§], *Gábor Galbács*[§], *Ákos Kukovecz*[†,φ], *Zoltán Kónya*[†,Ψ]

[†]Department of Applied and Environmental Chemistry, University of Szeged, H-6720 Szeged, Hungary

[Φ]MTA-SZTE "Lendület" Porous Nanocomposites Research Group, University of Szeged, H-6720 Szeged, Hungary

[ψ]Department of Physical Chemistry and Material Science, University of Szeged, H-6720 Szeged, Hungary

[§]Department of Inorganic and Analytical Chemistry, University of Szeged, H-6720 Szeged, Hungary

[Ψ]MTA-SZTE Reaction Kinetics and Surface Chemistry Research Group, University of Szeged, H-6720 Szeged, Hungary

ABSTRACT: 6.6 nm Pt nanoparticles with narrow size distribution were anchored on mostly identical, amorphous silica supports (SBA-15, MCF-17, Silica Foam) and were tested in ethanol decomposition reactions at < 300 °C. The reaction on the Pt/SBA-15 was ~2 times faster (0.073 molecules·site^{-1}·s^{-1}) compared to Pt/MCF-17 (0.042 molecules·site^{-1}·s^{-1}) and Pt/SF (0.040 molecules·site^{-1}·s^{-1}) at 300 °C. In the case of Pt/SF, selectivity towards acetaldehyde was ~2 times higher compared to the Pt/MCF-17 and Pt/SBA-15 catalysts. In the case of Pt/MCF-17 and Pt/SBA-15, the methane to acetaldehyde ratio was ~ 4 times higher compared to the Pt/SF catalyst. The ethene selectivity was ~1.5 times higher in the case of Pt/SBA-15 compared to Pt/MCF-17 and Pt/SF. Small Angle X-ray Scattering (SAXS) studies showed striking differences in the nature of the surface of the different silica supports, which may be responsible for the activation, and selectivity deviation in ethanol decomposition reactions. The SBA-15 has the most disordered mesostructure and SF has a fine surface structure with a diffuse phase boundary may resulted in the high activity and varying selectivity, respectively.

INTRODUCTION

Mesoporous silica-based catalyst supports are common in both industry and research due to their high specific surface area and ordered pore structure. In silica-based catalysts, some metal-support interactions (sintering[1], encapsulation[2], alloy-formation[3], inter-diffusion[4] etc.) can arise at elevated temperatures[5] evidenced by regular surface analyzing techniques (Transmission Electron Microscopy, Low Energy Electron Diffraction, X-ray Photoelectron Spectroscopy etc.);

however, at moderate conditions these supports are relatively inert due to their irreducible nature. Are they really inert?

Due to the inertness, these oxides are frequently used for reference state supports in heterogeneous catalytic test reactions. The hydrogenation of crotonaldehyde over silica supported Pt nanoparticles showed that the silica has no active role in the reaction. Titania supported catalyst showed higher activity and selectivity compared to Pt supported on mesoporous silica[6]. In CO oxidation over Pt nanoparticles anchored onto the surface of several mesoporous metal-oxides, mesoporous silica (MCF-17) was used as a comparative support[7].

On the other hand, silica materials are covered by weak acidic silanol groups, which are catalytically inert. However, the surface hydroxyl density has an effect on the charge transfer and the adhesion of the metal[8,9]. Additionally, we know that the metal-silica interface plays an important role in catalysis as CeO_2-Pt-SiO_2 tandem catalyst show activation in ethylene hydroformilation reaction where Pt-CeO_2-SiO_2 system was inactive[10].

In the present work we give an account of the decomposition of ethanol on several almost identical silica based supported Pt catalysts, with particular emphasis on the effects of the supports. We focused on the comparison of three similarly structured, zeotype mesoporous silica materials namely MCF-17, SBA-15 and Silica Foam (SF). MCF-17 is a member of the Mesostructure Cellular Foam (MCF) family with a three-dimensional (3D) structure with ultra-large (>20 nm) and robust mesopores. SBA-15 has uniform hexagonally ordered pores with narrow size distribution[11], while SF is a mesoporous silica with a disordered structure.

6.6 nm Pt nanoparticles with controlled size were deposited on SBA-15, MCF-17 and SF supports and were tested in ethanol decomposition at 100-300 °C in the gas phase. The ethanol decomposition on the Pt/SBA-15 was ~2 times faster (0.073 molecules$\cdot$site$^{-1}\cdot$s^{-1}) compared to

Pt/MCF-17 (0.042 molecules·site^{-1}·s^{-1}) and Pt/SF (0.040 molecules·site^{-1}·s^{-1}) at 300 °C. In the case of Pt/SF, selectivity towards acetaldehyde was ~2 times higher compared to the Pt/MCF-17 and Pt/SBA-15 catalysts. We found similarities between the silica supports and derived catalysts with powder X-ray Diffraction (XRD) and N_2 sorption techniques. All silica based supports are highly amorphous with a mesoporous structure and a high specific surface area. Besides the regular surface characterization methods, Small Angle X-ray Scattering (SAXS) studies showed striking differences in the porosity, pore- and mesostructure, as well as the surface fine structure which may be responsible for the catalytic activity and selectivity risen from the different nature of Pt-SiO_2 interfaces of the different silica supports.

RESULTS & DISCUSSION

Characterization of the silica supports, Pt nanoparticles and supported catalysts

MCF-17, SBA-15 and Silica Foam (SF) mesoporous silica supports were synthesized successfully by a soft template method from tetraethyl orthosilicate (TEOS) precursor (*see Supporting Information for details*)[12-14]. MCF-17 mesoporous silica has tetragonal-shape wall building blocks and is determined by a hexagonally ordered mesostructure where the thickness of the walls are 2-4 nm and the pore diameter is 20-30 nm (*Fig. 1/A.*). In the case of SBA-15, linearly ordered pores are characteristic where the average pore diameter as well as the wall thickness is 4-5 nm (*Fig. 1/B.*). Mainly, the ends of the pores are open, however capping and reversals are also presented. In the case of SF silica, the average diameter of the pores is 4-9 nm, where the wall thickness is ~ 2-4 nm. SF silica is built of randomly situated tiny and porous silica building blocks linked together (*Fig. 1/C.*).

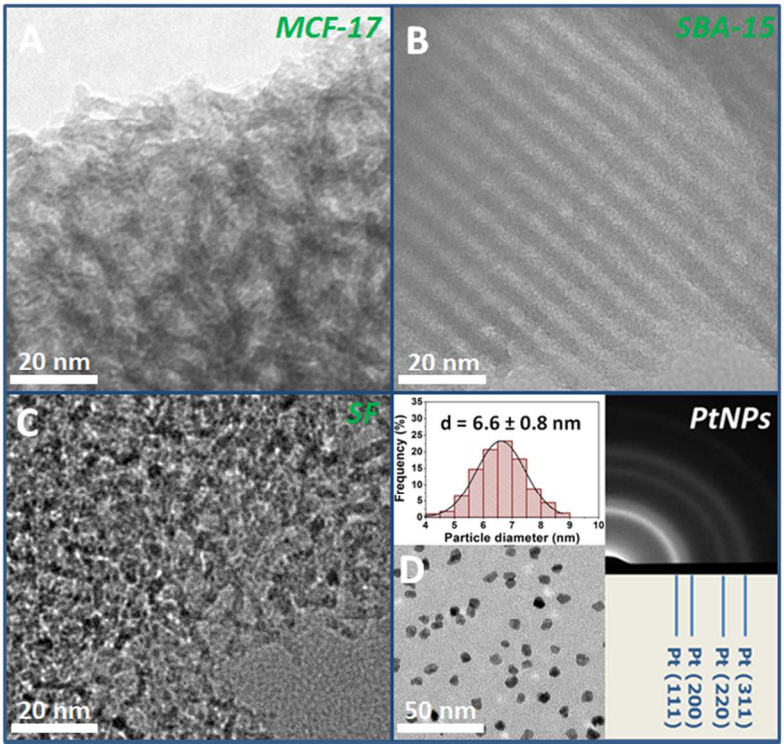

Figure 1. Typical TEM images of (A) MCF-17, (B) SBA-15 and (C) SF silica supports as well as (D) 6.6 ± 0.8 nm metallic Pt nanoparticles with narrow size distribution (ED pattern shows the presence of metallic Pt).

The Pt nanoparticles were synthesized by the polyol method from platinum-based salt precursor using polyvinylpyrrolidone (PVP) as a capping agent and ethylene glycol as a reducing agent and the media for the reaction. The as-prepared Pt nanoparticles have narrow size distribution with an average diameter of 6.6 ± 0.8 nm (*Fig. 1/D.*). Electron Diffraction patterns confirms the presence of Pt (111), Pt (200), Pt (220) and Pt (311) crystallite planes characteristic for metallic face-centered cubic (fcc) Platinum.

For comparing the effect of the different silica support in heterogeneous catalysis, the as-prepared 6.6 nm Pt nanoparticles were deposited onto the surface of MCF-17, SBA-15 and SF

with a loading of 1.1-1.3 wt%. The Pt nanoparticles show an even surface coverage with a well-defined distribution on the surface of the silica supports (*Fig. S1.*).

Ethanol decomposition reaction over 6.6 nm Pt nanoparticles supported on MCF-17, SBA-15 and SF silica supports

The as-prepared catalysts were tested in thermal decomposition of ethanol in the gas phase at 100-300 °C (*Fig 2.*) as this reaction has industrial importance as well as reaction kinetics research interest. The mechanism is based on two main pathways towards ethene (dehydration) and acetaldehyde (dehydrogenation) and one side pathway through the decomposition of acetaldehyde towards methane and carbon-monoxide (*Scheme 1.*).

Scheme 1. The reaction pathways for ethanol decomposition towards acetaldehyde, methane and carbon-monoxide and ethene

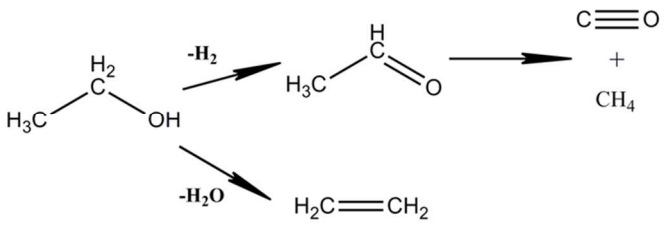

The ethanol decomposition on the Pt/SBA-15 was ~2 times faster (0.073 molecules·site^{-1}·s^{-1}) compared to Pt/MCF-17 (0.042 molecules·site^{-1}·s^{-1}) and Pt/SF (0.040 molecules·site^{-1}·s^{-1}) at 300 °C (*Fig. 2/A.*). On the most active catalyst (Pt/SBA-15) the decomposition starts above 200 °C and ~4 % conversion was reached at 300 °C.

In the case of Pt/SF, selectivity towards acetaldehyde was ~2 times higher (55%) compared to the Pt/MCF-17 (29%) and Pt/SBA-15 (25%) catalysts (*Fig. 2/B.*). In the case of Pt/MCF-17 and

Pt/SBA-15, the methane to acetaldehyde ratio was 2.44 and 2.97, respectively, while it was ~ 4 times lower (0.70) for Pt/SF catalyst. The selectivity towards ethene was insignificant in the case of all silica based catalysts, however the ethene selectivity was ~1.5 times higher in the case of Pt/SBA-15 (0.30%) compared to Pt/MCF-17 (0.21%) and Pt/SF (0.23%). In summary, Pt/SBA-15 are the most active catalysts, however SF supported catalysts produces acetaldehyde with the highest selectivity, while Pt nanoparticles anchored onto the surface of MCF-17 and SBA-15 form methane with the highest selectivity.

In all cases, hydrogen, acetaldehyde, carbon-monoxide and ethene were produced. At higher temperatures the amount of acetaldehyde decreased, and those of ethene and methane increased. Selectivity towards hydrogen (calculation based on the total hydrogen input) for all silica supported Pt catalysts reach the highest value at > 220 °C (*Fig. 2/C.*). All catalysts are produces hydrogen with a similar selectivity.

After the catalytic tests up to 300 °C, the deactivation of the silica supported catalysts were monitored at 300 °C for 4 hours (*Fig. 2/D.*). The catalysts were continuously deactivated during the catalyst aging process. In the case of the Pt/SBA-15, Pt/MCF-17 and Pt/SF the activation decrease to 65 %, 42 % and 23 %, respectively.

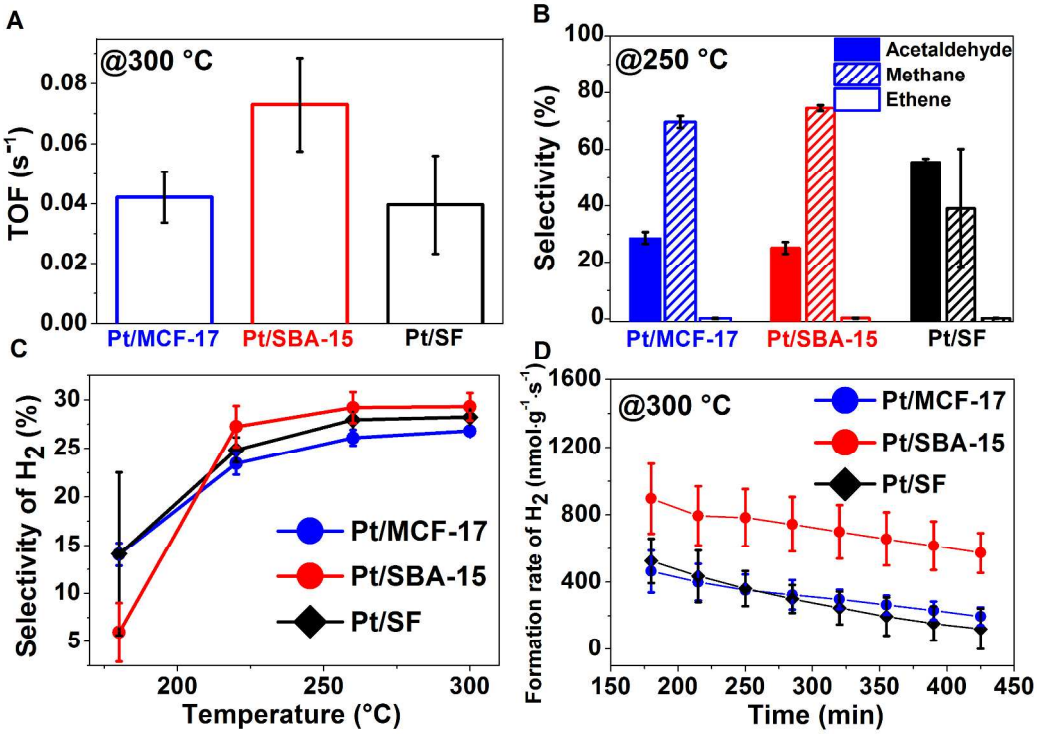

Figure 2. Ethanol decompostion to methane, acetaldehyde and ethene over MCF-17, SBA-15 and SF supported 6.6 nm Pt nanoparticles at 100 – 300 °C. (A) The turnover frequency of the Pt nanoparticles supported on the different silicas at 300 °C, (B) The selectivity towards acetaldehyde, methane and ethene at 250 °C, (C) The hydrogen selectivity in the range of 150-300 °C and (D) the deactivation of the catalysts at 300 °C.

Meso- and Surface Fine Structure Study based on Small Angle X-ray Scattering & N_2 Adsorption Isotherms

Several methods are known for the characterization of the structural and surface properties of nano-structured materials, mainly based on adsorption[15-19] or photoelectron scattering[20-21] methods. These methods are based on the connection between the surface roughness and the fractal dimensions[22] and the results from the different investigation methods are usually in good agreement, however, significant differences can be also possible[23].

Small Angle X-ray Scattering (SAXS) (*see Supplementary Information for details*) as well as surface fractal calculation based on the N_2 adsorption isotherms[18] was used to obtain structural and surface information about the different silica supports. Pt loaded catalysts before and after the ethanol decomposition reaction were also investigated by SAXS.

The log-log plot (fractal plot) of the SAXS profiles for SBA-15, MCF-17 and SF silica supports presented differences in the ordering, packing, meso- and surface fine structure of the mesoporous materials (*Fig. 3/A*). The SBA-15 silica shows a strong (100) and two weak (110) and (200) peaks (the ratio of the values belonging to the peaks is $1:\sqrt{3}:2$), implying a high degree of two-dimensional hexagonal (P6mm) structure[24]. The *d*-spacing calculated via the equation of $d_{100} = 2\pi/h_{100}$, and the unit cell parameter $a = 2d_{100}/\sqrt{3}$ are $d_{100} = 8.9$ *nm* and $a = 10.3$ *nm*, which values are in good agreement with the pore and wall distances observed on the TEM images (*Fig. 1/B.*). Similarly, the SAXS pattern of MCF-17 exhibits a primary and some higher-ordered peaks with decreasing intensities that suggests typical cellular foam mesostructure[25]. For SF silica support, no significant ordering was observed which is in agreement with the TEM images of SF (*Fig.1/C*).

The surface fractal dimension values resulted from the fractal-plot gives information about the surface roughness properties of the materials (*Table S1.*). In the case of MCF-17 (D_S=1.95) and SF (p=1.7), the object has a compact structure with an insignificant surface roughness and sharp or diffuse phase boundary, respectively (Fig. 4.). However, SBA-15 shows ~1.5-2 times higher surface fractal dimension value (D_S=3.2) compared to MCF-17 and SF showing a loose structure with a significant rough surface characteristic for surface fractal type structures in the micro- and meso-scale regime of 0.3-5 nm.

Surface fractal dimensions determined based on the adsorption isotherms of the silica supports (*Fig. 3/B.*) shows similar roughness tendencies compared to the SAXS measurements. The surface roughness was the highest for SBA-15 (D_s=2.73) compared to MCF-17 (D_s=2.64) and SF (D_s=2.43). The differences in the surface fractal dimension values were also reported by Malekani et al[23].

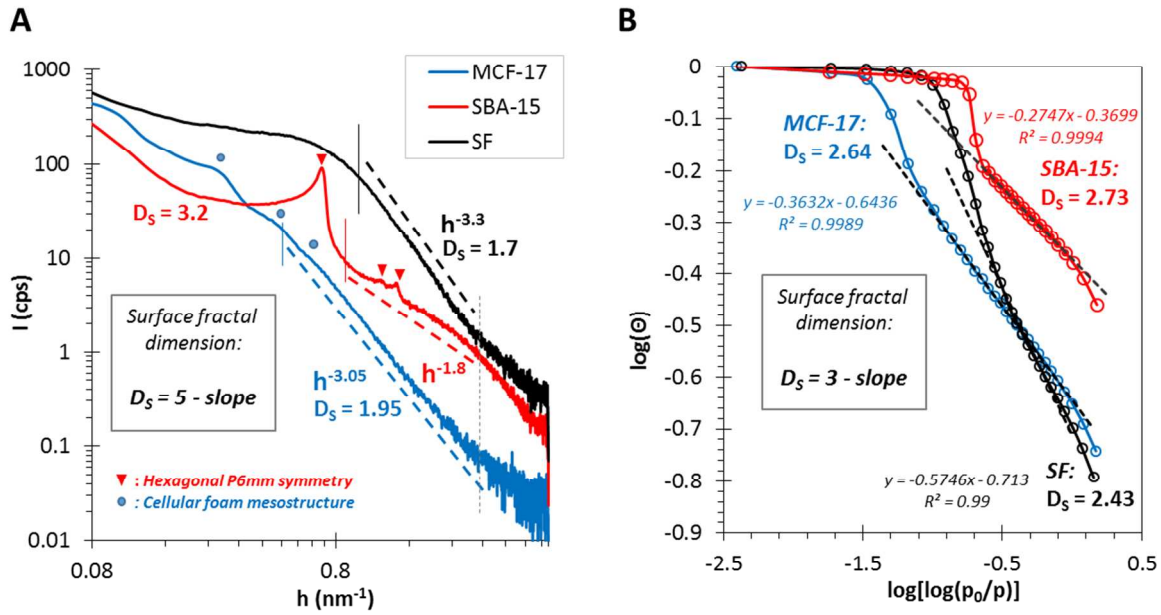

Figure 3. (A) The fractal plot of the Small Angle X-ray Scattering (SAXS) curves of the MCF-17, SBA-15 and SF supports. (dashed lines indicate the power-law exponents for calculating the surface fractal dimensions; the vertical lines indicate the validity range of the power-law.) (B) Logarithmic plot of the adsorption isotherms for the MCF-17, SBA-15 and SF samples to determine the surface roughness (equations of the linear trend lines and the calculated surface fractal dimensions are indicated.)

The fractal plot as well as the calculation based on the N_2 adsorption isotherms gives reliable information about the quality of the surface roughness with a quantitative information based on

the surface fractal dimensions (D_s=2 presents smooth surface, while D_s=3 denote for rough surface). In the case of the SAXS studies, applying the Porod plot instead of the fractal plot, gives information about the nature (sharp or diffuse phase boundary or electron density fluctuation) as well as the dimension of the surface inhomogeneity can be determined (*Fig. S2 and Table S1*). Considering to the Porod plots of pure MCF-17, SBA-15 and SF (*Fig. 4/A.*), it can be established that in the case of MCF-17 the fitted curve has no significant deviation from a flat slope which fact suggests a sharp phase boundary in between the pores and the walls resulted in a smooth silica surface in the nanometer scale (*Fig. 4/B.*). For SBA-15 silica, the positive slope indicates the presence of small scattering centers as well as sharp electron density fluctuations, which are the result of the highly rough surface. In the case of the SF silica, the negative slopes show the presence of diffuse phase boundary which can be attributed to the highly amorphous nature of the support evidenced by TEM and XRD studies (*Fig. S3.*). The differences of the silica supports may resulted in different amount as well nature of surface hydroxyl groups which has an effect of the total surface charge as well as the number of Pt-silica bonds[8]. As the Pt-SiO_2 interface[9] as well as the surface roughness[19] plays an important role in heterogeneous catalytic reactions and the lack of sintering of the Pt nanoparticles during the catalytic process (Fig. S1.), the striking differences in the nature of the surface of the different silica supports can be responsible for the activation and selectivity deviation in ethanol decomposition reactions. The high mesostructured roughness of the SBA-15 may resulted in the high catalytic activity, as well as the diffuse phase boundaries may be responsible for the selectivity differences observed at SF-based catalysts in ethanol decomposition reactions. As the amount of surface hydroxyl group

MCF-17, SBA-15 and SF supports loaded with 6.6 nm Pt nanoparticles before and after the ethanol decomposition reaction were also subjected to SAXS investigations (*Fig. S4.*). The

surface fractal properties as well as the nature of the surface roughness of MCF-17, SBA-15 and SF samples change negligibly with the anchoring of the Pt nanoparticles and no other changes are observed after the catalyst were tested in ethanol decomposition reaction.

The calculated specific surface area values based on the K_p/Q value by SAXS are in good agreement with data obtained from nitrogen sorption measurements using the Brunauer-Emmett-Teller theory[26] (BET measurements) based on the Barrett-Joyner-Halenda (BJH) method[27] (*Table S1.*). The wall thickness (L_s) resulted from the inhomogeneity length of the structure for MCF-17, SBA-15 and SF were 8.3 nm, 5.7 nm and 2.7 nm, respectively, which is in agreement with the broadened SiO_2 (101) diffractions at $2\Theta = 23°$ of the XRD studies (*Fig. S3/A.*) and the TEM images of the pure silica supports (*Fig. 1.*).

The pore diameters (L_p) were 30.7 nm for MCF-17, 8.5 nm for SBA-15 and 4.7 nm for SF before the deposition of the Pt nanoparticles. These values are in good agreement with the TEM studies, however in case of MCF-17 the pore size calculated from the BET studies was smaller. The E value (the length of the inhomogeneity at the interfaces) was showing the amount of the extent of the surface fine structure calculated from the Porod plot. These value is almost 1.5 times higher for SBA-15 (1.27 nm) compared to the SF support (E = 0.83 nm).

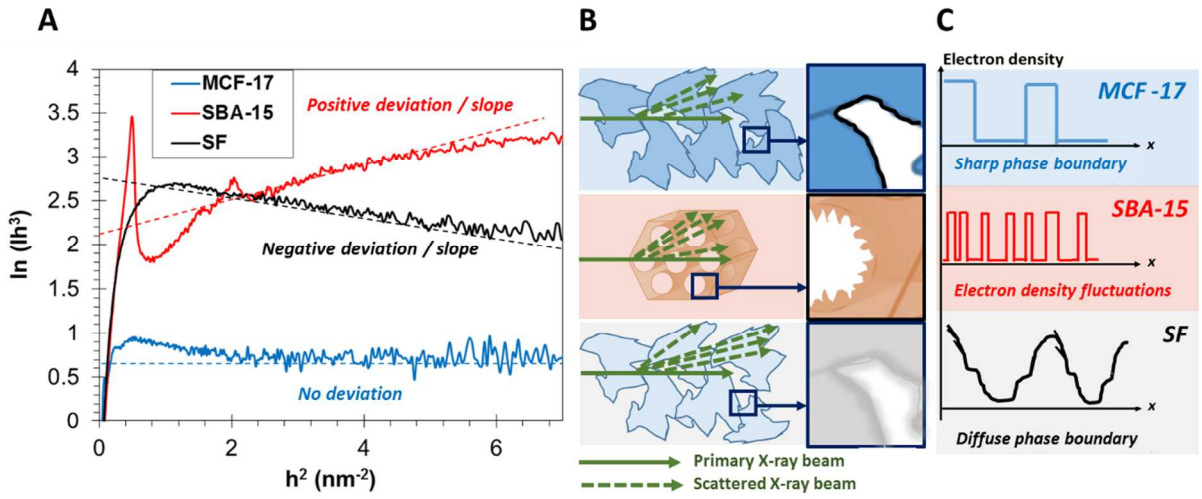

Figure 4. (A) Porod-plot of the Small Angle X-ray scattering (SAXS) curves of MCF-17, SBA-15 and SF silica supports. (B) Schematic view of the X-ray scattering angle for the silica supports and the fine structure of the surfaces represents the nano-scaled physical differences corresponding to the different catalytic activity and selectivity of the Pt/SiO_2 catalysts. (C) Schematic view of the electron density differences resulted from the SAXS measurements.

Investigation of the MCF-17, SBA-15 and SF Silica Supports by N_2 Adsorption, X-ray Diffraction & Transmission Electron Microscopy

Beside the SAXS measurements, the samples were investigated by regular physico-chemical techniques used in surface chemistry and heterogeneous catalysis. Powder XRD studies of MCF-17, SBA-15 and SF in the range of 2Θ = 10-80° show the absence of highly intensive peaks for all the silica supports (*Fig. S3/A.*). The only presence of a broadened SiO_2 (101) diffraction at 2Θ = 23° with low intensity indicate amorphous silica based catalyst supports. In the case of the MCF-17, this diffraction was more significant compared to SBA-15 and SF.

The N_2 adsorption/desorption studies of the supports show isotherms with hysteresis loop characteristic for mesoporous materials (*Fig. S3/B.*). The shapes of the isotherms for all supports

are similar, however, in the case of the SBA-15, type IV isotherm shape are observed, while MCF-17 and SF are grouped into the mesoporous materials with type V isotherms[28]. The difference is mild however we may conclude that the surface of the SBA-15 shows a stronger adhesion with the adsorbent molecules compared to MCF-17 and SF which may be also responsible for the higher activity of the Pt/SBA-15 catalyst. In the case of SBA-15 and SF, the hysteresis loop of type H1 showing the ordered structure of the material. For MCF-17, type H2 characteristic can be fitted showing the presence of some structural disorder in the material. The specific surface areas are 518 $m^2 \cdot g^{-1}$, 798 $m^2 \cdot g^{-1}$ and 666 $m^2 \cdot g^{-1}$ for MCF-17, SBA-15 and SF, respectively (*Table S1.*).

The pore size distribution for MCF-17 is monodisperse showing an average pore diameter of 3.9 nm with a total pore volume of 0.9 $cm^3 \cdot g^{-1}$. In the case of SBA-15, the average pore diameter was 4.2 nm with a total pore volume of 0.8 $cm^3 \cdot g^{-1}$. SF support showed a broadened size distribution of the pore diameter (3-9 nm) with an average of 4.6 nm. The total pore volume was ~50% higher (1.3 $cm^3 \cdot g^{-1}$) compared to the other silica based supports. In summary, the SBA-15 has higher specific surface area (20-50 %), however the SF supports showed the highest total pore volume.

The anchoring of the 6.6 nm Pt nanoparticles onto the different silica supports was successful. Mostly single Pt particles are presented in the case of MCF-17, SBA-15 and SF (*Fig. S1.*). After the catalyst pretreatment in oxygen and hydrogen at 300 °C and after the ethanol decomposition reaction at 100-300 °C, the sintering of adjacent nanoparticles was not observed. The size of the Pt nanoparticles stayed in the regime of 6.1 – 6.7 nm. In case of the SBA-15, the surface diffusion of the Pt nanoparticles was occurred resulted in clusters of 4-5 nanoparticles on the surface after the catalytic reaction. It is well known that Pt nanoparticles with different diameters can

show different activity and selectivity in heterogeneous catalytic reactions[29]. In this study, no significant sintering was observed may exclude a strong effect of Pt shape and size on the different catalytic activity and selectivity.

CONCLUSION

In this study, three zeo-type silica supports (MCF-17, SBA-15 and SF) were synthesized with similar chemical and different pore and wall structure. 6.6 nm Pt nanoparticles were anchored on the surface of the supports and the as-prepared catalysts were tested in ethanol decomposition reactions in the gas phase at <300 °C. The reaction on the Pt/SBA-15 was ~2 times faster (0.073 molecules·site^{-1}·s^{-1}) compared to Pt/MCF-17 (0.042 molecules·site^{-1}·s^{-1}) and Pt/SF (0.040 molecules·site^{-1}·s^{-1}) at 300 °C. In the case of Pt/SF, selectivity towards acetaldehyde was ~2 times higher (55%) compared to the Pt/MCF-17 (29%) and Pt/SBA-15 (25%) catalysts. In the case of Pt/MCF-17 and Pt/SBA-15, the methane to acetaldehyde ratio was ~ 4 times higher compared to the Pt/SF catalyst.

SBA-15, MCF-17 and SF are amorphous mesostructured silicas with high specific surface area. SAXS studies showed striking differences in the surface, porosity, the pore- and mesostructure of the silica supports as well as the Pt nanoparticles decorated catalysts. MCF-17 and SBA-15 has ordered mesostructure, while SF is disordered. There is also a striking difference in the surface fine structure of the different silica supports. In the case of MCF-17, a smooth silica surface was dominant. However, for SBA-15 silica, the small scattering centers as well as sharp electron density fluctuations are resulted from the special pore structure (pore-matter alteration). In the case of SF silica, diffuse phase boundary was presented. As the Pt-SiO_2 interface plays an important role in heterogeneous catalytic reactions, we believe that the striking differences in the

nature of the surface of the different silica supports can be responsible for the activation and selectivity deviation in ethanol decomposition reactions. We believe that the high activity of SBA-15 supported Pt nanoparticle catalyst can be attributed to the high mesostructured roughness of the support. In the case of SF-based catalyst, The diffuse phase boundaries may be responsible for the significant selectivity differences compared to MCF-17 and SBA-15 supported catalysts.

In this study, we support the idea that the silica has a striking effect on the activity and selectivity of the catalysts in heterogeneous catalytic reactions and we also demonstrated new evidences of surface effects by SAXS studies in addition to the TEM, XRD, BET methods. In the future, we will focus on the exact connection between meso- and surface fine structure by SAXS and surface chemical processes such as catalytic performance.

ASSOCIATED CONTENT

Supporting Information.

Detailed experimental procedures and supplementary figures and table. This material is available free of charge via the Internet at http://pubs.acs.org.

AUTHOR INFORMATION

Corresponding Author

* sapia@chem.u-szeged.hu

Author Contributions

‡These authors contributed equally.

ACKNOWLEDGMENT

This paper was supported by the János Bolyai Research Scholarship of the Hungarian Academy of Sciences and the ÚNKP-ÚNKP-16-4 New National Excellence Program of the Ministry of Human Capacities as well as the Hungarian Research Development and Innovation Office through grants NKFIH OTKA PD 120877 of AS. DS, GH and ÁK are grateful for the fund of NKFIH (OTKA) PD 116224, NKFIH (OTKA) PD 115769, and NKFIH (OTKA) K112531 & NN110676, respectively. This collaborative research was partially supported by the "Széchenyi 2020" program in the framework of GINOP-2.3.2-15-2016-00013 "Intelligent materials based on functional surfaces – from syntheses to applications" project.

REFERENCES

(1) Hayasi, K.; Horiuchi, T.; Suzuki, T.; Mori, T. Sintering Behavior of Pt Metal Particles Supported on Silica-Coated Alumina Surface. *Catal. Lett.* **2002**, *78*, 43-47.

(2) Powell, B. R.; Whittington, S. E. Encapsulation: A new mechanism of catalyst deactivation. *J. Catal.* **1983**, *81*, 382-393.

(3) Kampshoff, E.; Walchli, N.; Kern, K. Silicide formation at palladium surfaces. Part I: Crystalline and amorphous silicide growth at the Pd(110) surface. *Surf. Sci.* **1998**, *406*, 103-116.

(4) Anton, R.; Neukirch, U.; Harsdorff, M. Auger-electron-spectroscopy analysis of a plasmon loss in palladium silicide formed from Pd deposits on silicon. *Phys. Rev. B* **1987**, *36*, 7422-7427.

(5) Min, B. K.; Santra, A. K.; Goodman, D. W. Understanding silica-supported metal catalysts: Pd/silica as a case study. *Catal. Today* **2003**, *85*, 113-124.

(6) Kennedy, G.; Baker, L. R.; Somorjai, G. A. Selective Amplification of C=O Bond Hydrogenation on Pt/TiO2: Catalytic Reaction and Sum-Frequency Generation Vibrational

Spectroscopy Studies of Crotonaldehyde Hydrogenation. *Angewandte Chemie* **2014**, *126*, 3405-3408.

(7) An, K.; Alayoglu, S.; Musselwhite, N.; Plamthottam, S.; Melaet, G.; Lindeman, A. E.; Somorjai, G. A. Enhanced CO Oxidation Rates at the Interface of Mesoporous Oxides and Pt Nanoparticles. *J. Am. Chem. Soc.* **2013**, *135*, 16689-16696.

(8) Ewing, C. S.; Veser, G.; McCarthy, J. J.; Karl Johnson, J.; Lambrecht, D. S. Effect of Support Preparation and Nanoparticle Size on Catalyst–Support Interactions between Pt and Amorphous Silica. *J. Phys. Chem. C* **2015**, *119*, 19934-19940.

(9) Ewing, C. .S.; Veser, G.; McCarthy, J. J.; Lambrecht, D. S.; Karl Johnson, J. Predicting catalyst-support interactions between metal nanoparticles and amorphous silica supports. *Surf. Sci.* **2016**, *652*, 278-285.

(10) Yamada, Y.; Tsung, C. K.; Huang, W.; Huo, Z.; Habas, S. E.; Soejima, T.; Aliaga, C. E.; Somorjai, G. A.; Yang, P. Nanocrystal bilayer for tandem catalysis. *Nat. Chem.* **2011**, *3*, 372-376.

(11) Li, Q.; Wu, Z.; Feng, D.; Tu, B.; Zhao, D. Hydrothermal Stability of Mesostructured Cellular Silica Foams. *J. Phys. Chem. C* **2010**, *114*, 5012-5019.

(12) Zhao, D. Y.; Huo, Q. S.; Feng, Y. L.; Chmelka, B. F.; Stucky, G. D. Nonionic Triblock and Star Diblock Copolymer and Oligomeric Surfactant Syntheses of Highly Ordered, Hydrothermally Stable, Mesoporous Silica Structures. *J. Am. Chem. Soc.* **1998**, *120*, 6024-6036.

(13) Schmidt-Winkel, P.; Lukens, W. W.; Yang, P.; Margolese, D. I.; Lettow, J. S.; Ying, J. Y.; Stucky, G. D. Microemulsion Templating of Siliceous Mesostructured Cellular Foams with Well-Defined Ultralarge Mesopores. *Chem. Mater.* **2000**, *12*, 686-696.

(14) Bagshaw, S. A. Morphosynthesis of macrocellular mesoporous silicate foams. *Chem. Comm.* **1999**, 767-768.

(15) Pfeifer, P.; Avnir, D. Chemistry in noninteger dimensions between two and three. I. Fractal theory of heterogeneous surfaces. *J. Chem. Phys.* **1983**, *79*, 3558-3565.

(16) Avnir, D.; Jaroniec, M. An isotherm equation for adsorption on fractal surfaces of heterogeneous porous materials. *Langmuir* **1989**, *5*, 1431-1433.

(17) Neimark, A.V.; Unger, K. K. Method of Discrimination of Surface Fractality. *J. Colloid Interf. Sci.* **1993**, *158*, 412-419.

(18) Prouzet, E; Boissiére, C.; Kim, S. S.; Pinnavaia, T. J. Roughness of mesoporous silica surfaces deduced from adsorption measurements. *Micropor. Mesopor. Mater.* **2009**, *119*, 9-17.

(19) Smith, A. M; Zoelle, A.; Yang, Y.; Rioux, R. M.; Hamilton, N. G; Amakawa, K.; Nielsen, P. K.; Trunschke, A. Surface roughness effects in the catalytic behavior of vanadia supported on SBA-15. *J. Catal.* **2014**, *312*, 170-178.

(20) Teixeira, J. Small-angle scattering by fractal systems. *J. Appl. Cryst.* **1988**, *21*, 781-785.

(21) Salinas-Nolasco, M. F.; Mendez-Vivar, J. Correlation between fractal dimension and surface characterization by small angle X-ray scattering in marble. *Langmuir* **2010**, *26*, 3889-3893.

(22) Avnir, D.; Biham, O.; Lidar, D.; Malcai, O. Is the Geometry of Nature Fractal? *Science* **1998**, *279*, 39-40.

(23) Malekani, K.; Rice, J. A.; Lin, J-S. Comparison of Techniques for Determining the Fractal Dimensions of Clay Minerals. *Clay. Clay. Miner.* **1996**, *44*, 677-685.

(24) Varga, N.; Benkő, M.; Sebők, D.; Bohus, G.; Janovák, L.; Dékány, I. Mesoporous silica core–shell composite functionalized with polyelectrolytes for drug delivery. *Micropor. Mesopor. Mat.* **2015**, *213*, 134-141.

(25) Xu, J.; Long, K. Z.; Chen, T.; Xue, B.; Li, Y. X.; Cao, Y. Mesostructured graphitic carbon nitride as a new base catalyst for the efficient synthesis of dimethyl carbonate by transesterification. *Catal. Sci. Technol.* **2013**, *3*, 3192-3199.

(26) Brunauer, S.; Emmett, P. H.; Teller, E. Adsorption of Gases in Multimolecular Layers. *J. Am. Chem. Soc.* **1938**, *60*, 309-319.

(27) Barrett, P. E.; Joyner, G. L.; Halenda, P. P. The Determination of Pore Volume and Area Distributions in Porous Substances. I. Computations from Nitrogen Isotherms. *J. Am. Chem. Soc.* **1951**, *73*, 373-380.

(28) Lowell, S.; Shields, J. E.; Thomas, M. A.; Thomess, M. *Characterization of Porous Solids and Powders: Surface Area, Pore Size and Density*; Springer: 2004

(29) Sapi, A.; Liu, F.; Xiaojun, C.; Thompson, C. M.; Wang, H.; An, K.; Krier, J. M.; Somorjai, G. A. Comparing the Catalytic Oxidation of Ethanol at the Solid–Gas and Solid–Liquid Interfaces over Size-Controlled Pt Nanoparticles: Striking Differences in Kinetics and Mechanism. *Nano Lett.* **2014**, *14*, 6727-6730.

TOC Graphic:

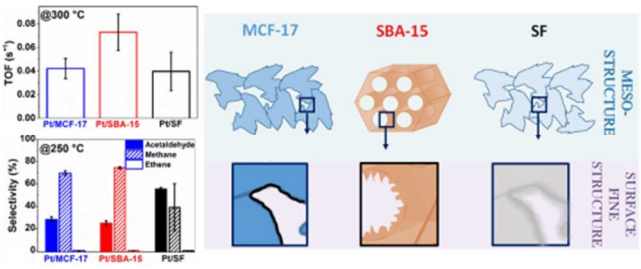

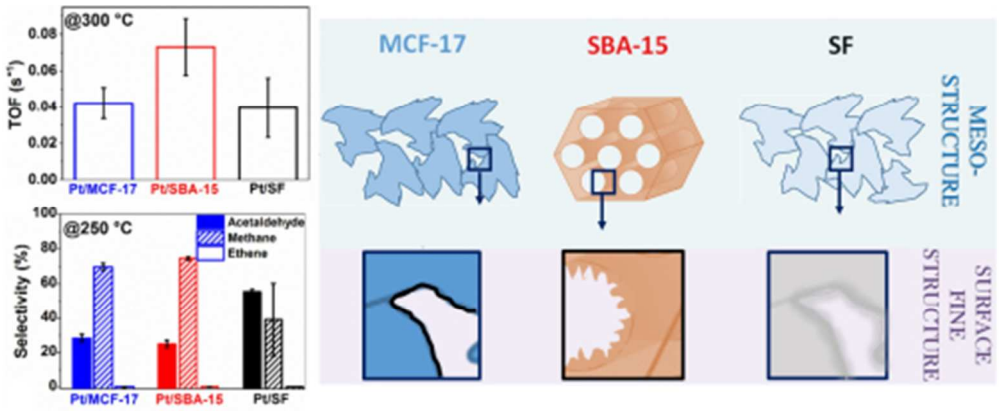

TOC graphic

85x34mm (150 x 150 DPI)